The University of Akron
IdeaExchange@UAkron

Chemical and Biomolecular Engineering Faculty Research

Chemical and Biomolecular Engineering Department

7-20-1993

Microemulsion Characterization by the Use of a Noninvasive Backscatter Fiber Optic Probe

Rafat R. Ansari

Harbans S. Dhadwal

Michael Cheung
University of Akron Main Campus, cheung@uakron.edu

William V. Meyer

Please take a moment to share how this work helps you through this survey. Your feedback will be important as we plan further development of our repository.
Follow this and additional works at: http://ideaexchange.uakron.edu/chemengin_ideas

 Part of the Chemistry Commons

Recommended Citation
Ansari, Rafat R.; Dhadwal, Harbans S.; Cheung, Michael; and Meyer, William V., "Microemulsion Characterization by the Use of a Noninvasive Backscatter Fiber Optic Probe" (1993). *Chemical and Biomolecular Engineering Faculty Research*. 5.
http://ideaexchange.uakron.edu/chemengin_ideas/5

This Article is brought to you for free and open access by Chemical and Biomolecular Engineering Department at IdeaExchange@UAkron, the institutional repository of The University of Akron in Akron, Ohio, USA. It has been accepted for inclusion in Chemical and Biomolecular Engineering Faculty Research by an authorized administrator of IdeaExchange@UAkron. For more information, please contact mjon@uakron.edu, uapress@uakron.edu.

Microemulsion characterization by the use of a noninvasive backscatter fiber optic probe

Rafat R. Ansari, Harbans S. Dhadwal, H. Michael Cheung, and William V. Meyer

This paper demonstrates the utility of a noninvasive backscatter fiber optic probe for dynamic light-scattering characterization of a microemulsion comprising sodium dodecyl sulfate/1-butanol/brine/heptane. The fiber probe, comprising two optical fibers precisely positioned in a stainless steel body, is a miniaturized and efficient self-beating dynamic light-scattering system. Accuracy of particle size estimation is better than ±2%.

Key words: Dynamic light scattering, fiber optic sensors, particle sizing, microemulsions, fuels, quasi-elastic light scattering.

1. Introduction

A. Microemulsions

Microemulsions are clear, thermodynamically stable dispersions of two immiscible liquids with carefully adjusted emulsifiers (surfactants and cosurfactants). The cosurfactants are normally short chain alcohols. The globule size of the dispersed phase is normally less than 1 μm. Oil-in-water, bicontinuous, and water-in-oil (W/O) microemulsion systems can be obtained on changing the solution environment by altering salinity or the concentration of a surfactant.[1,2]

One difficulty in studying critical microemulsions has been stratification[2] and hydrodynamic instabilities[3] that are due to gravity. This gravity sensitivity is not completely unexpected as there are experimental[4–7] and theoretical[8,9] indications that the very low free energy differences between states with significantly different microstructures can lead to substantial composition variations in microemulsions, especially in the middle phase. Further, microdroplet clustering is believed to precede phase separation in some cases,[10] leading to local density differences between the disperse and the continuous phases on a length scale large enough to promote stratification. The physical–chemical state of the microemulsions remains a subject of discussion because of questions of polydispersity and shape of the droplets, surface properties of the electrically charged droplets in ionic systems, droplet–droplet interactions, the effect of pH on phase behavior, and the role of the interfacial film because of surfactants and cosurfactants.

One of the most sought-out physical characteristics of a microemulsion system is the globule size in the case of a monodisperse system and the globule size distribution in the case of a polydisperse system. The expected size range is in the submicrometer regime, and therefore dynamic light scattering (DLS) techniques are very appropriate for experimental characterization of microemulsions.[1] There are many textbooks on the subject of light scattering and the interested reader should consult Ref. 11 for a historical perspective of the subject and Ref. 12 for understanding the practice of DLS.

B. Review of Backscatter Fiber Optic Systems

The first backscatter fiber optic system, a fiber optic Doppler anemometer (FODA), was described by Dyott in 1978.[13] The FODA was successfully developed into a compact and portable single-angle DLS system for use in the sizing of colloidal suspensions[14,15] and for the routine characterization of the motility of bovine spermatozoa.[16] The FODA represented a significant break from conventional DLS systems by enclosing the transmitting and the receiving optics into a T-shaped metal housing, which was mounted directly onto a helium neon laser. Transmitted and scattered laser light was guided to and from the

R. R. Ansari and W. V. Meyer are with NASA Lewis Research Center/Case Western Reserve University, Mail Stop 105-1, 21000 Brookpark Road, Cleveland, Ohio 44135-3191. H. S. Dhadwal is with the Department of Electrical Engineering, State University of New York at Stony Brook, Stony Brook, New York 11794-2350. H. M. Cheung is with the Department of Chemical Engineering, The University of Akron, Akron, Ohio 44325-3906.

Received 30 September 1992.
0003-6935/93/213822-06$06.00/0.
© 1993 Optical Society of America.

scattering region through a single multimode optical fiber. Separation of the transmitted and scattered signals was achieved by means of a hole-in-mirror beam splitter mounted into the T-shaped housing. The FODA provided a homodyne detection of the scattered light in the backward direction (180° ± 4.5°). The local oscillator was derived from the phase mismatch at the fiber–liquid interface. The FODA successfully demonstrated the utility of fiber optics for making DLS accessible to clinical–industrial environments. Additionally, the free end of the fiber was dipped directly into the scattering system, consistent with clinical–industrial requirements, as demonstrated in the measurements carried out on bovine spermatozoa for the artificial insemination program.[17]

Auweter and Horn[18] modified the FODA by replacing the hole-in-mirror beam splitter with a multimode fiber optic directional coupler. In 1991, Dhadwal[19] reported a backscatter fiber optic probe, which utilized separate optical fibers for transmitting and receiving, thereby eliminating the need for a beam splitter. Homodyne detection was achieved through the use a gradient-index microlens positioned in contact with two fibers, which were placed side by side. As discussed by Dhadwal *et al.*[20] and Thomas,[21] the single-fiber backscatter systems (homodyne) exhibit unreliability and ambiguity in the estimation of size from concentrated suspensions; this arises because of the lack of knowledge of the relative strength of the local oscillator to scattered signal strength. In order to overcome this difficulty, a more efficient and compact backscatter fiber optic probe, which provided a self-beating detection of the scattered light, was developed.[20] The self-beating fiber optic probe comprises two optical fibers positioned side by side, but mounted into a common ferrule. The fiber probe was designed for direct immersion into the scattering medium. The accuracy and reliability of this probe was demonstrated over a range of aqueous concentrations of several different standards of polystyrene latex spheres (PLS's). Dhadwal and Ansari[22] also developed another type of self-beating backscatter fiber optic probe, which provided simultaneous access to a range of scattering angles in the backward direction. In particular, a linear array of fibers was positioned in the back focal plane of a gradient-index microlens. One of the fibers was used for delivering a Gaussian laser beam to the scattering region, while the remaining fibers provided access to 10 backscatter angles separated by 2.2°.

There are many potential applications that could benefit from the use of a backscatter fiber optic probe, but require noninvasive interrogation. Single-fiber backscatter systems (homodyne) are not suitable for positioning outside sample containers, but the self-beating probe, comprising two separate optical fibers, can be modified for this purpose. As shown in Fig. 1, the two optical fibers, in addition to being displaced in the transverse direction, can also be tilted with respect to each other. This added degree of freedom allows precise location of the edge of the scattering region from the tip of the probe body, thereby enabling the fiber probe to be positioned outside the scattering cell. With this added feature, the backscatter fiber optic probe provides access to odd-shaped and remotely located scattering cells. We have successfully applied the noninvasive backscatter probe to the study of cataractogenesis in excised but intact human[23] and bovine[24] eye lenses, and low molecular weight protein systems in the dilute regime.[25]

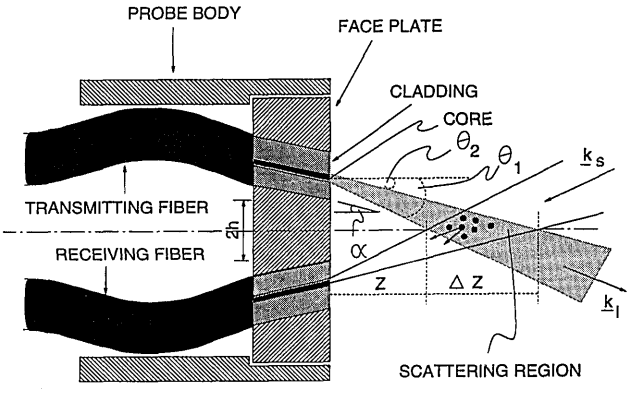

Fig. 1. Schematic of a noninvasive lensless backscatter fiber optic probe. θ is the scattering angle, k_I and k_s are the incident and scattering wave vectors, respectively; $|k_I| = |k_s| = 2\pi/\lambda_0$, where λ_0 is the free-space wavelength of the laser source.

In this paper we demonstrate the utility and the effectiveness of a noninvasive fiber probe to perform DLS study on a microemulsion system. This preliminary investigation establishes the important role of noninvasive backscatter fiber optic probes. A typical microemulsion system is characterized by several phases, and the precise location of each phase may not always be known *a priori*. In order to study the dynamics of such systems by the use of DLS, an optical apparatus with the capability of interrogating the stratified column, without disturbing the microemulsion, is required. A conventional DLS system with distributed and bulky transmitted and receiving optics, would require considerable modification to meet this challenge. In contrast, a noninvasive backscatter probe, as described below, is ideally suited for such applications.

2. Noninvasive Backscatter Fiber Optic Probe

The requirements of a noninvasive backscatter fiber optic probe are more demanding than those of an immersible filter probe. The noninvasive fiber probe must illuminate and interrogate a small volume in the interior region of a scattering vessel while providing self-beating detection; strong backreflections from the scattering vessel must not enter the receiving fiber. Figure 1 shows a schematic of a lensless noninvasive backscatter fiber probe body, which consists of a cylindrical stainless steel tube with a matching faceplate. Two optical fibers are epoxied into precisely drilled holes in the face plate. Separation h and inclination α between the two holes define

scattering angle θ, and edge of the scattering region Z, from the fiber probe tip and the length of the scattering region ΔZ. One of the fibers is used for illuminating the scattering region with a diverging Gaussian laser beam, while the second optical fiber, together with a photomultiplier connected to the other end of the fiber, provides a self-beating detection of laser light scattered in the backward direction.

The challenge in the design of a backscatter fiber optic probe lies in determining the optimum pair of values for h and α that provide acceptable estimates of particle size from the measured intensity–intensity autocorrelation data and that are consistent with required values of Z and ΔZ. Assuming that the two optical fibers are identical, the following set of equations, which governs the design of the fiber probe, can be derived by geometric arguments:

$$Z = \left[h + \frac{D_f}{2\cos(\alpha)}\right]\frac{1}{\tan(\theta_1)}, \quad (1)$$

$$\Delta Z = \left[h + \frac{D_f}{2\cos(\alpha)}\right]\left[\frac{1}{\tan(\theta_2)} + \frac{1}{\tan(\theta_1)}\right], \quad (2)$$

$$\theta = \pi - 2\sin^{-1}[(n_1/n_2)\sin(\alpha)], \quad (3)$$

$$\sin(\theta_1) = (n_1/n_2)\sin(\alpha + \rho), \quad (4)$$

$$\sin(\theta_2) = (n_1/n_2)\sin(\alpha - \rho), \quad (5)$$

$$\rho = \cos^{-1}(n_3/n_1), \quad (6)$$

where D_f is the core diameter of the optical fiber; θ_1 and θ_2 are determined by the numerical aperture of the optical fiber and the refractive index of the scattering medium n_2; and n_1 and n_3 are the refractive indices of the core and the cladding of the optical fiber, respectively. From the above set of equations, it can be ascertained that a self-beating, lensless, and noninvasive fiber optic probe can be designed to meet a range of challenging experimental conditions. For example, it is possible to fabricate a fiber probe capable of providing measurements of the scattered light at 90°, without the use of any other optical components. From the above equations, we have fabricated a backscatter lensless fiber optic probe with a nominal scattering angle of 143° in aqueous solutions, $Z \approx 3$ mm, and $\Delta Z < 1$ mm. The waist of the Gaussian laser beam exiting from the fiber probe has a waist radius of 2 μm. It is appropriate to note at this point that there may be some applications for which delivery of a focused laser beam is critical. This issue is discussed by Dhadwal *et al.*[26] in a paper in this feature issue. That paper discusses the integration, through fusion splicing, of a gradient-index fiber lens to a monomode optical fiber, before it is mounted into the faceplate. The process of fusion splicing and subsequent cleaving is still being perfected.

3. Experimental Procedure

A. Sample Preparation

Our experiments employed a three-phase microemulsion system comprising sodium dodecyl sulfate (SDS)/1-butanol/brine/heptane. Details on this system can be found elsewhere.[27] SDS (98%), 1-butanol [99.9+%, high-performance liquid chromatography (HPLC) grade], n-heptane (99+%, HPLC grade), and NaCl [99.9+%, American Chemical Society reagent grade) were obtained from Aldrich Chemical Company and, aside from filtering stock solutions, were used as received. Water was de-ionized and filtered (0.2 μm) as supplied and was again thrice filtered (0.2 μm) before use. Samples were prepared from 20 wt. % SDS and NaCl stock solutions, heptane, water, and 1-butanol. The SDS and NaCl stock solutions and water were thrice filtered through a 0.2-μm filter to remove dust. The heptane and 1-butanol were used as received. The HPLC-grade 1-butanol and n-heptane were filtered by the manufacturer (0.5 μm). The A-series microemulsions consist of equal weight fractions of a 6.54 wt. % NaCl brine and n-heptane and varying percentages of a surfactant mixture. The surfactant mixture is composed of SDS and 1-butanol in the mass ratio 1:2. The compositions are provided in mass percent in Table 1. The samples were prepared in 13-mm Kimax screw-cap test tubes that had been repeatedly rinsed with thrice-filtered (0.2-μm) water and then dried. The sealed samples were equilibrated for a minimum of 24 h before use.

B. Experimental Setup

The experimental setup, which is described elsewhere,[20] requires coupling of light into the transmitting monomode optical fiber and a photomultiplier for the detection of photons collected by the receiving optical fiber. A 20× microscope objective was used to couple light from a He–Ne laser source (NEC Model GLG 5261), with a peak power of 5 mW, to the monomode optical fiber. Optical power emanating from the probe tip was adjusted to ~1 mW in order to establish a lower threshold for operation of the fiber probe DLS system. Figure 2 shows a photograph of the fiber probe interrogating a microemulsion column.

Table 1. Composition of A-Series Microemulsion Samples

Sample	Surfactant Mixture	6.54 wt. % NaCl Solution	Heptane
A0	1.00	49.50	49.50
A1	3.00	48.50	48.50
A2	5.00	47.50	47.50
A3	7.00	46.50	45.50
A4	9.00	45.50	45.50
A5	11.00	44.50	44.50
A6	13.00	43.50	43.50
A7	15.00	42.50	42.50
A8	17.00	41.50	41.50
A9	20.00	40.00	40.00

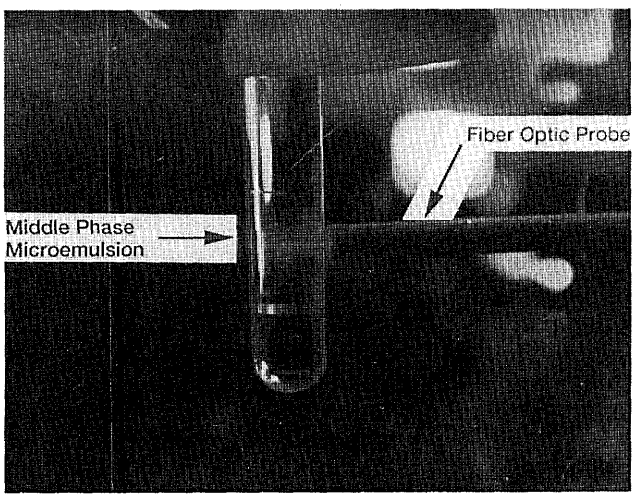

Fig. 2. Photograph showing the fiber probe interrogating the microemulsion system.

A conventional DLS system (Brookhaven Instruments Corporation Model BI-2000SM), operating at a wavelength of 514.5 nm with a power level of 400 mW, was used to make measurements of the intensity–intensity autocorrelation on the same set of samples. Photoelectron pulses from either the fiber system or the BI-200SM were correlated with a digital correlator (Brookhaven Instruments Corporation Model BI2030). Intensity–intensity autocorrelation data from 10 microemulsion samples were measured for a 300-s duration with both systems discussed above.

C. Data Analysis

In a typical DLS experiment the measured intensity–intensity autocorrelation $G^{(2)}(t_m)$, and the normalized first-order electric-field autocorrelation $g^{(1)}(t_m)$, are related through the Siegert relation,

$$G^{(2)}(t_m) = A[1 + \beta|g^{(1)}(t_m)|^2], \tag{7}$$

where A is an estimate of the baseline, t_m is the delay time of the mth channel, and β is a measure of the self-beating efficiency, with a maximum value of unity.

The first-order electric-field autocorrelation is given by a Laplace transform of the distribution of diffusion coefficients $G(D)$, that is,

$$\sqrt{\beta}g^{(1)}(t_m) = \left[\frac{G^{(2)}(t_m)}{A} - 1\right]^{1/2} = \sqrt{\beta}\int_{D_{\min}}^{D_{\max}} G(D)\exp(-Q^2Dt_m)\mathrm{d}D, \tag{8}$$

where $Q = (4n\pi/\lambda_0)\sin^2(\theta/2)$ is the Bragg wave number, n is the refractive index of the suspension medium, λ_0 is the free-space wavelength of the coherent light source, θ is the scattering angle, and $D_{\min}$ and $D_{\max}$ are the lower and upper bounds, respectively, on the diffusion coefficient D. The diffusion coefficient is related to radius r of spherical particles through the Stokes–Einstein equation,

$$D = \frac{kT}{6\pi\eta r}, \tag{9}$$

where k is Boltzmann's constant, T is the absolute temperature, and η is the solvent viscosity.

Data analysis involves inversion of the Laplace transform expressed in Eq. (8) to obtain $G(D)$, or a characteristic linewidth distribution $G(\Gamma)$, with $\Gamma = Q^2D$. This inversion procedure is ill conditioned in the presence of noise, which is unavoidable in the accumulation of data. Many techniques for solving this inversion problem are in existence. The reader is referred to Chu's textbook[12] for a detailed account of these procedures. Subsequent to obtaining $G(\Gamma)$, the particle size distribution can be recovered through a scaling process involving Eq. (9) and knowledge of the scattering amplitude for each of the species in suspension.

The autocorrelation data in this paper has been analyzed by the use of a cumulant expansion of the kernel in Eq. (8), as described by Koppel,[28] and by the use of a nonnegative least-squares technique, as described by Lawson and Hanson.[29]

4. Results and Discussion

An aqueous suspension of PLS's (obtained from Bang Laboratories) with nominal diameters of 85 nm and a weight concentration of 0.05% was prepared as described in Ref. 26. Ten 60-s duration intensity–intensity autocorrelations were measured by the fiber probe system and analyzed by a third-order cumulant analysis.[28] The results, summarized in Table 2, show that the accuracy of recovering the particle diameter is better than ±2%. Additionally, as expected, the overall polydispersity factor is fairly small, and the nominal self-beating factor is 0.86.

Table 2. Summary of the Third-Order Cumulants Analysis of Autocorrelation Data Obtained From 0.05% by Weight Concentration Polystyrene Latex Spheres of 85-nm Nominal Diameter[a]

Run Number	β	Particle Diameter (nm)	Polydispersity
1	0.86	87.4	0.005
2	0.86	85.7	0.005
3	0.86	89.2	0.005
4	0.87	86.3	0.005
5	0.86	88.4	0.005
6	0.87	85.6	0.055
7	0.87	85.9	0.067
8	0.86	87.9	0.005
9	0.86	87.3	0.005
10	0.86	85.1	0.005

[a]These measurements were taken with the fiber probe system. Polydispersity is a measure of the ratio of the standard deviation to the square of the mean.

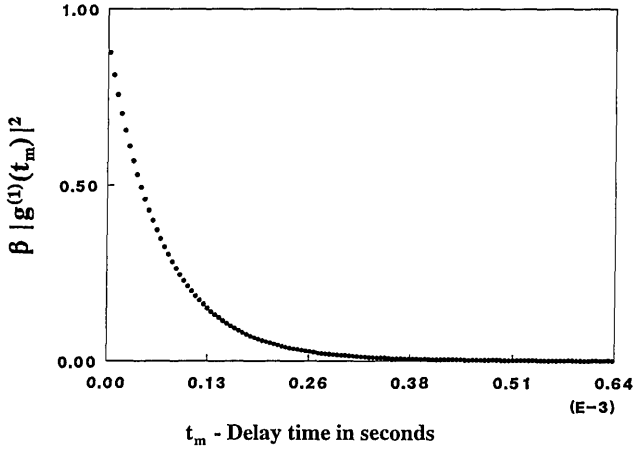

Fig. 3. Normalized intensity–intensity autocorrelation function obtained from the lower phase microemulsion (sample A3). $g^{(1)}(t_m)$ is the first-order electric-field autocorrelation, t_m is the time of the mth delay channel, and β is the self-beating efficiency factor.

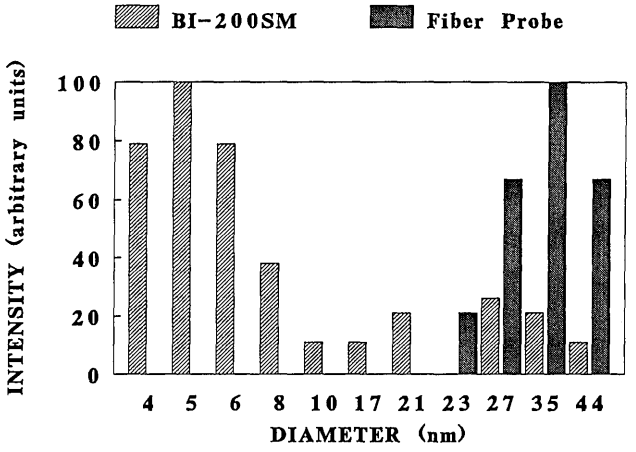

Fig. 5. Comparison of the particle size distributions recovered, by the use of a nonnegative least-squares curve fitting,[29] from a concentrated dispersion (10 wt. %) of 39-nm PLS's. Both measurements were made at a scattering angle of 143°.

The 10 samples of microemulsion classified in Table 1 were characterized by the use of both the backscatter fiber optic probe and the BI-200SM system. Figure 3 shows a normalized intensity–intensity autocorrelation we obtained from sample A3 using the fiber probe. We used a third-order cumulant analysis to analyze the autocorrelation data obtained from all 10 samples. Figure 4 shows a comparison of the average globule diameter of the microemulsion in the various phases. Solid diamonds and solid triangles correspond to data we obtained using the fiber system and the BI-200SM system, respectively. There is good agreement between measurements made in the lower- and middle-phase microemulsions, with the exception of sample A4. Samples A8 and A9, in the upper phase, exhibit differences in the estimates of the globule diameter.

Microemulsions are transparent solutions, but because of their high-volume fractions, they may exhibit multiple light scattering (MLS) effects. In the dispersions of PLS's, MLS effects are pronounced at higher particle concentrations.[20,21] The BI-200SM system gave lower estimates of particle size, consistent with MLS effects.[21] In order to confirm that this discrepancy is due to MLS, we prepared a 10% weight concentration of an aqueous dispersion of PLS's with nominal diameters of 35 nm. Autocorrelation data obtained with both the fiber probe and the BI-200SM were analyzed by a nonnegative least-squares procedure supplied by the digital correlator. Figure 5 shows a comparison of the size distributions recovered from the autocorrelation data. The BI-200SM system was also used at a scattering angle of 143°. As expected,[21] the backscatter fiber probe gives very reasonable estimates of the particle size at these high concentrations. The BI-200SM, as would any other conventional DLS system, gives particle size estimates that are lower than expected. Microemulsion samples A8 and A9, as indicated in Table 1, have high surfactant concentrations of 17 and 20 wt. %, respectively. If we interpret a high surfactant concentration as producing similar effects as a high concentration of PLS, as discussed above, then MLS accounts for the discrepancy between the size estimates shown in Fig. 5.

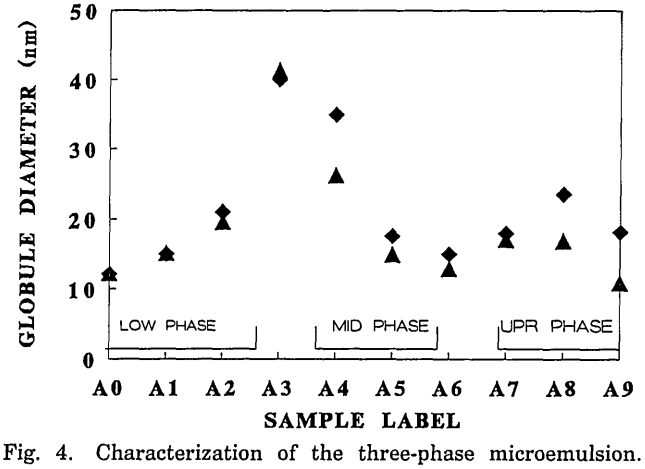

Fig. 4. Characterization of the three-phase microemulsion. Globule diameter is determined by a third-order cumulants analysis[28] of the autocorrelation data. Solid diamonds and solid triangles represent measurements made with the fiber probe and with the BI-200SM system, respectively.

5. Conclusion

In this paper we have used a noninvasive backscatter fiber optic probe to characterize a microemulsion system consisting of SDS/1-butanol/brine/heptane. Our DLS optical system has a unique design that does not require any lenses, has no moving parts, does not need alignment, is insensitive to vibrations, and mitigates the problems of MLS.

The authors thank NASA's Microgravity Sciences and Applications Division, Code SN, and Thomas K. Glasgow of the Processing Science and Technology Branch of the NASA Lewis Research Center for their support of this work. H. S. Dhadwal and H. M.

Cheung acknowledge the research support from grants NCC-3241 and NAG3-906, respectively.

References

1. A. A. Calj'e, W. G. M. Agterof, and A. Vrij, "Light scattering of concentrated W/O microemulsion; Application of modern fluid theories," in *Micellization, Solubilization, and Microemulsions,* K. L. Mittal, ed. (Plenum, New York, 1976), Vol. 2, pp. 779–790.
2. B. Pouligny and F. Nallet, "Free surface instability and stratification of critical microemulsions," Europhys. Lett. **6,** 341–347 (1988).
3. L. Quentela, N. Fernandex, J. Quiben, D. Losada, and C. Ferreiro, "Nonequilibrium phenomena in critical microemulsions," Progr. Colloid Polym. Sci. **76,** 165–168 (1988).
4. J. J. Rosen and Z.-P. Li, "The nature of the middle phase in three-phase micellar systems at phase behavior optimal salinity," J. Colloid Interface **97,** 456–464 (1984).
5. F. Zhao, M. J. Rosen, and N-L. Yang, "Spin probe studies of the microviscosity gradient in the middle phase of three-phase micellar systems," Colloids Surf. **11,** 97–108 (1984).
6. R. J. Good, J. T. Ho, G. E. Groers and X. Yang, "The anomaly of sedimentation at normal gravity in microemulsion," J. Colloid Interface **107,** 290–292 (1985).
7. R. J. Good, J. T. Ho, G. E. Groers, and X. Yang, "Sedimentation in middle phase microemulsions: an investigation using light scattering and ultracentrifugation," Colloids Surf. **20,** 187–209 (1986).
8. Y. Jeng and C. A. Miller, "Theory of microemulsions with spherical drops. I. Phase diagrams and interfacial tensions in gravity free systems," Colloids Surf. **28,** 247–269 (1987).
9. J. Jeng and C. A. Miller, "Theory of microemulsions with spherical drops. II. Effects of gravity," Colloids Surf. **28,** 271–288 (1987).
10. A. M. Ganz and B. E. Boeger, "Fluorescence method for observing clustering of microemulsion droplets near the critical point," J. Colloid Interface Sci. **109,** 504–507 (1986).
11. B. Chu, ed., *Selected Papers on Quasielastic Light Scattering by Macromolecular, Supramolecular, and Fluid Systems,* Vol. MS12 of SPIE Milestone Series (Society of Photo-Optical Instrumentation Engineers, Optical Engineering Press, Bellingham, Wash. 1990).
12. B. Chu, *Laser Light Scattering: Basic Principles and Practice* (Academic, New York, 1991).
13. R. B. Dyott, "The fiber optic Doppler anemometer," Microwave Opt. Acoust. **2,** 13–18 (1978).
14. D. A. Ross, H. S. Dhadwal, and R. B. Dyott, "The determination of the mean and standard deviation of the size and distribution of a colloidal suspension of submicroscopic particles using the fibre optic Doppler anemometer, FODA," J. Colloid Interface Sci. **64,** 533–542 (1978).
15. H. S. Dhadwal and D. A. Ross, "Size and concentration of particles in Syton using the fibre optic Doppler anemometer, FODA," J. Colloid Interface Sci. **76,** 478–489 (1980).
16. D. A. Ross, H. S. Dhadwal, and J. A. Foulkes, "Laser measurement of the motility of bull spermatozoa in an egg yolk diluent," J. Reprod. Fertil. **67,** 263–268 (1983).
17. J. G. Bullock and D. A. Ross, "The measurement of sperm motility by fibre optic Doppler anemometer as prediction of bovine fertility," Lasers Opt. Eng. **4,** 39–53 (1983).
18. H. Auweter and D. Horn, "Fibre-optical quasi-elastic light scattering studies of concentrated dispersions," J. Colloid Interface Sci. **105,** 399–409 (1985).
19. H. S. Dhadwal, "A back scatter fiber optic probe for particle sizing," in *Gradient-Index Optical Systems,* Vol. 9 of 1991 OSA Technical Digest Series, (Optical Society of America, Washington, D.C., 1991), pp. 165–167.
20. H. S. Dhadwal, R. R. Ansari, and W. V. Meyer, "A fiber optic probe for particle sizing in concentrated systems," Rev. Sci. Instrum. **63,** 2963–2968 (1991).
21. J. C. Thomas, "Fiber optic dynamic light scattering from concentrated dispersions. 2. Concentration dependence of the apparent diffusion coefficient," Langmuir **5,** 1350–1355 (1989).
22. H. S. Dhadwal and R. R. Ansari, "A multiple fiber optic probe for several applications," in *Fiber Optic and Laser Sensors IX,* R. P. DePaula and E. Udd, eds., Proc. Soc. Photo-Opt. Instrum. Eng. **1584,** 262–272 (1991).
23. H. S. Dhadwal, R. R. Ansari, and M. A. DellaVecchia, "A coherent fiber optic sensor for early detection of cataractogenesis in a human eye lens," Opt. Eng. **32,** 233–238 (1993).
24. R. R. Ansari, H. S. Dhadwal, M. A. DellaVecchia, and M. Campbell, "A fiber optic sensor for ophthalmic refractive diagnosis," in *Fiber Optic Medical and Fluorescent Sensors and Applications,* D. R. Hansmann, F. P. Milanovich, G. G. Vurek, and D. R. Walt, eds., Proc. Soc. Photo-Opt. Instrum. Eng. **1648,** 83–105 (1992).
25. H. S. Dhadwal, W. Wilson, R. Ansari, and W. V. Meyer, "Dynamic light scattering studies of BSA and Lysozyme using a backscatter fiber optic system," in *Fiber Optic Medical and Fluorescent Sensors and Applications,* D. R. Hansmann, F. P. Milanovich, G. G. Vurek, and D. R. Walt, eds., Proc. Soc. Photo-Opt. Instrum. Eng. **1648** (to be published).
26. H. S. Dhadwal, R. R. Khan, and K. Suh, "Integrated fiber optic probe for dynamic light scattering," Appl. Opt. (to be published).
27. J. Van Nieuwkoop, R. B. De Boer, and G. Snoei, "Microemulsion phase relationships in the system sodium dodecyl sulphate/1-butanol/brine/heptane," J. Colloid Interface Sci. **109,** 350–363 (1986).
28. D. E. Koppel, "Analysis of macromolecular polydispersity in intensity correlation spectroscopy: the method of cumulants," J. Chem. Phys. **57,** 4814–4820 (1972).
29. C. L. Lawson and R. J. Hansen, *Solving Least Squares Problems* (Prentice-Hall, Englewood Cliffs, N.J., 1974).